AIAA SciTech Forum
6-10 January 2025, Orlando, FL
AIAA SCITECH 2025 Forum

10.2514/6.2025-1234

An Experimental Investigation on the Aerodynamic Performance Degradation due to Ice Accretion Near the Tip Regions of Offshore Wind Turbines

Harsha Sista[1], Jincheng Wang[2], Anvesh Dhulipalla[3], Haiyang Hu[4], Hui Hu[5]
Department of Aerospace Engineering, Iowa State University, Ames, Iowa, 50011

With the recent rise in the installation of wind turbines, extreme weather conditions such as heavy rainfall and icing weather have been found to affect the performance of wind turbines seriously. Offshore wind turbines are especially affected because of the addition of sea spray icing. The added water will increase the overall Liquid Water Content (LWC) as the turbine blade rotates towards the ocean, resulting in two distinct icing regimes: in-cloud icing at the top of the rotation circle, and sea-spray icing at the bottom. In the present study, experiments are conducted to quantify the effects of high liquid water content (LWC) conditions at the tip region of an offshore wind turbine blade using advanced flow diagnostic techniques. The aerodynamic performance degradation of the turbine blade is first studied through dynamic measurements of the lift and drag force while high-speed imaging captures the dynamic ice accretion process. Consequently, Particle Image Velocimetry is then used to capture the change in the flow field around the airfoil model as the ice builds up. Different LWC values and temperature values are tested to cover the entire spectrum of offshore wind turbine icing conditions, including glaze ice, mixed ice, and rime ice.

1. Introduction

The rise of renewable energy has been accelerated in the 21st century, with wind and solar energy at the forefront of this change. Wind Energy is one of the fastest growing renewable energy sources, and has seen widespread adoption both onshore and offshore [1]. Offshore Wind Turbines have been an up-and-coming asset in the renewable energy portfolio for the last couple of decades. With the energy policy of Europe and North America focusing on expanding the percentage of energy generated through renewable energy, offshore wind has seen heavy investment and exponential growth [2], [3]. The United States aims to have a 30 Gigawatt installed offshore wind energy capacity by 2030, which has seen a rapid rise in commercial offshore wind farms [4]. Due to this increase in the demand and viability of wind energy, the installation of offshore wind turbines in cold climate regions has risen. Wind turbines in cold climates present a unique set of challenges, which has been summarized in a study by Lehtomaki [5]. It was found that 72%, 94% and 19% of onshore wind turbines suffer from icing events in North America, Europe and Asia respectively. These numbers will only be exaggerated for offshore turbines, but there is a lack of concrete data to quantify the extent of the effect of ice accumulation on the turbine blades. In addition, turbine maintenance is more challenging in an offshore setting. It is known that ice accumulation on the surfaces of wind turbine blades can change their shapes and decrease their aerodynamic performance, which can account for up to 30% of the Annual Energy Production (AEP)[6], [7]. With respect to offshore wind turbines, because of the presence of sea spray icing, the added water will result in different ice shapes. Since wind turbines depend on the generated lift force to carry on their rotational cycle, performance degradation due to ice accretion in extreme cases can cause the turbines to cut off and stop rotating. Therefore, it is crucial to study the aerodynamic performance degradation as a result of icing at higher Liquid Water Content (LWC) values to quantitatively understand how much offshore wind turbine icing affects the aerodynamic forces. In particular, the tip region of the wind turbine blade will experience the highest LWC values since it is susceptible to both in-cloud icing as well as sea spray icing. Therefore, the tip region of a typical offshore wind turbine is used in this study.

[1] PhD Student, Department of Aerospace Engineering.
[2] PhD Student, Department of Aerospace Engineering.
[3] PhD Student, Department of Aerospace Engineering.
[4] Post-Doctoral Researcher, Department of Aerospace Engineering.
[5] Martin C. Jischke Professor, Dept. of Aerospace Engineering, AIAA Associate Fellow. Email: huhui@iastate.edu

2. Experimental Setup and Test Model

The experimental study was performed in the unique Icing Research Tunnel available at Iowa State University (i.e., ISU-IRT in short), which is a newly refurbished, multifunctional icing research tunnel. As shown schematically in Fig. 1, ISU-IRT has a test section with four optically transparent side walls and dimensions of 2.0m in length x 0.4m in width x 0.4m in height. It has a capacity of generating a maximum wind speed of 100 m/s and airflow temperature down to - 25ºC. An array of pneumatic atomizers/spray nozzles (H. Ikeuchi and Co., Flat Spray BIMV Series Nozzles) were installed at the entrance of the contraction section of ISU-IRT to generate the droplets. The ISU-IRT is currently capable of generating LWC up to 10.0 g/m^3. The LWC can be adjusted by changing the air and water pressure and the supplied flow rate. By using ISU-IRT, extensive icing and anti-/de-icing studies have been carried out in recent years for various engineering applications. Further information about the ISU-IRT can be found in Gao et al. [8] and Hu et al. [9].

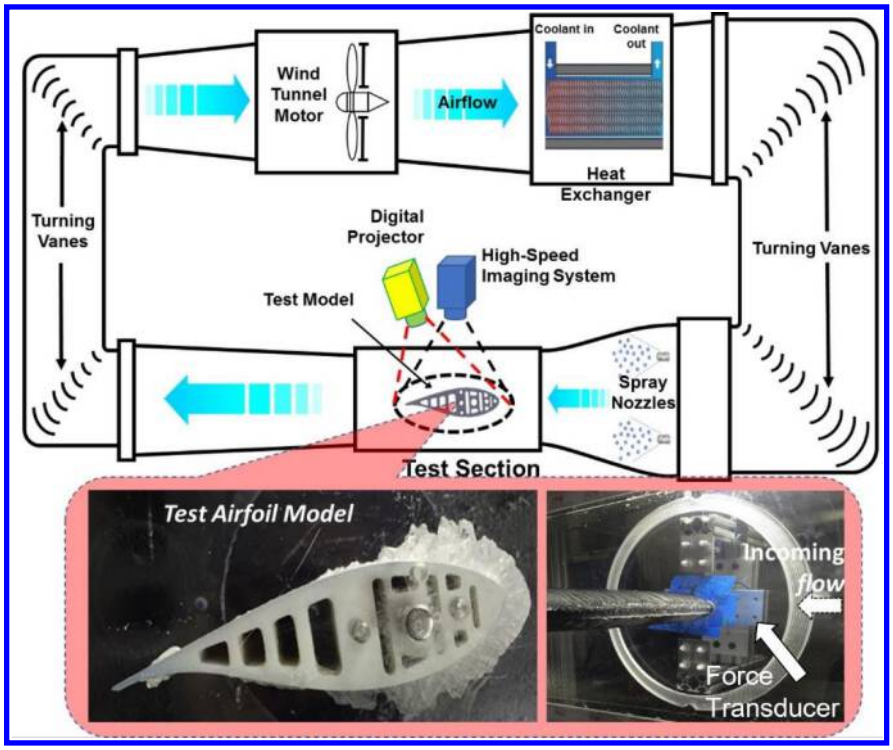

Figure 1: Schematic of the ISU-IRT

The airfoil model used in the experimental study is the FFA-W3-211 airfoil profile, which is the recommended airfoil to be used in the 15-MW Offshore Reference Wind Turbine proposed by the International Energy Agency [10]. The FFA-W3 series airfoils were developed by the Technical University of Denmark (DTU), and have desirable aerodynamic characteristics, and their geometries are publicly available for use. A turbine blade model was manufactured using this airfoil profile, is 0.15m in airfoil chord length (i.e., C ¼ 0.15 m) and 0.40m in spanwise length. The blade was mounted using a stainless-steel rod and set at an Angle of Attack of 8.0 degrees (i.e., AOA=5.0°), which coincides with the angle at which the airfoil model has its maximum lift-to-drag ratio. The typical tip speed experienced by currently installed offshore wind turbines can range from 50-70 m/s, with the promise of being faster as the turbines get bigger. Therefore, to simulate typical glaze icing conditions experienced by offshore wind turbines, the initial testing parameters were set to V_∞ = 60 m/s, T_∞ = 5 ºC. The ice accretion was studied for 3 different test cases with LWC = 1.0 g/m^3, LWC = 3.0 g/m^3 and LWC = 6.0 g/m^3, to capture the various icing conditions expected in the tip of an offshore wind turbine. A high-speed imaging system was used to capture the dynamic ice accretion process for these test cases. Two multi-axis force-moment transducers (ATI-IA Mini 45) are mounted on either end of the blade in order to measure the unsteady aerodynamic forces of lift and drag acting on the model during the dynamic ice accretion process.

The ambient air inside the test section and the wind turbine blade model are cooled down with the help of the heat exchanger to the target temperature, which is below the freezing point of water. The spray system in the ISU-IRT is then turned on, and the supercooled water droplets are carried towards the test section by the incoming airflow. When these supercooled water droplets impinge on the airfoil surface, they freeze at the leading edge, forming a layer of ice as time goes on. For glaze ice, when the temperatures are relatively warm, the latent heat of fusion released by the phase change is not taken away completely by heat transfer and some portion of the droplet remains in the liquid state. This portion is driven back by the aerodynamic shear stress, freezing in stages further downstream.

A high-resolution Particle Image Velocimetry (PIV) system was also used to achieve flow field measurements over the airfoil surface. PIV is a flow visualization technique popularly used in fluid dynamics research to obtain instantaneous velocity contours. The Nd: YAG laser (Evergreen) has a wavelength of 532 nm, and is used as an illumination source for the tracer particles. Smoke particles ~ 1μm in diameter are used for the dry measurements before the spray is turned on, while the water droplets from the spray nozzle system, which have a Median Volume Diameter (MVD) of ~ 20 μm are used for the rainfall cases. A series of convex and concave cylindrical lenses and optical mirrors were used to generate the laser sheet, which was perpendicular to the airfoil model, illuminating the mid-span region. A high-speed camera (Photron Fastcam Mini) was used in conjunction with a digital delay generator (Berkeley Nucleonics, Model 565) to coordinate the timing of the laser illumination and the image acquisition. The PIV setup is shown in Fig. 2:

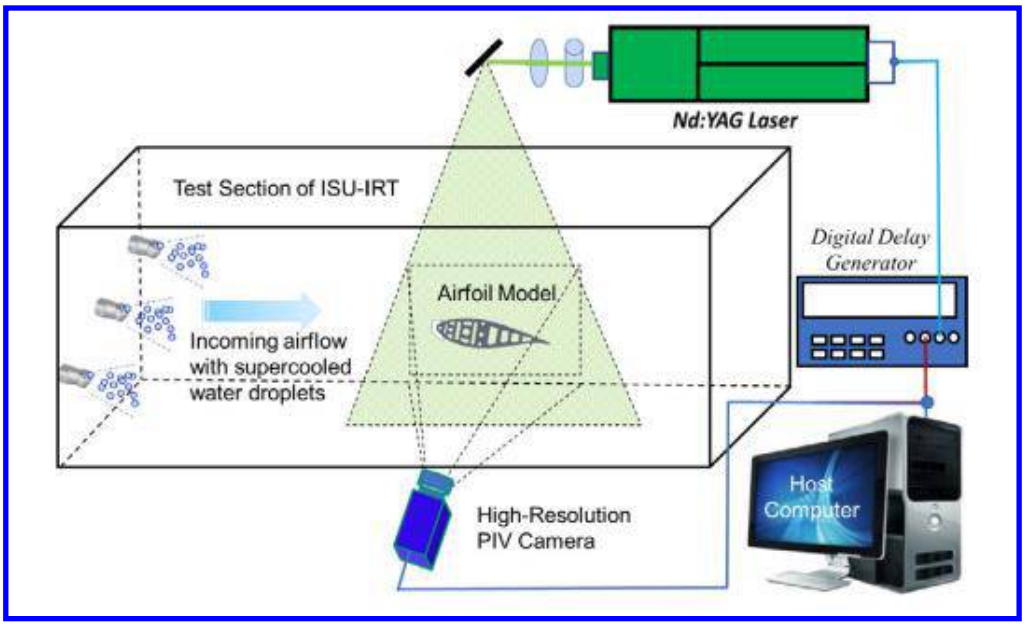

Figure 2: Experimental Setup for PIV measurements.

3. Measurement Results and Discussions

3.1 High-Speed Imaging Results

The high-speed imaging results for the glaze icing cases are shown below in Fig. 3. We can observe that in Fig. 3 (a), for the LWC = 1.0 g/m^3 case, the ice freezes around the leading edge, and there is no runback observed. We also see the leading-edge ice thickness increase as time goes on. In Fig. 3(b), for the LWC = 3.0 g/m^3 case, the ice does not freeze completely around the leading edge; instead, we observe runback where the incoming water freezes in stages. This is because the latent heat of fusion is not completely taken away by the ambient air. We also see the leading-edge ice thickness increase as time goes on, but the ice is spread out fairly evenly, both above and below the leadings edge. In Fig. 3 (c), for the LWC = 6.0 g/m^3 case, we observe much more runback, both in terms of the quantity and the chordwise extension of the rivulets. This results in a decrease in the amount of ice accreting around the leading edge. Therefore, even though we see a slight increase in the leading-edge ice thickness, most of the ice is actually on the surface of the airfoil in the form of runback rivulets. Therefore, we see the correlation established through previous work that the leading-edge ice thickness decreases with an increase in the LWC value [11].

The high-speed imaging results for the rime icing cases are shown below in Fig. 4. We can observe that in Fig. 4 (a), for the LWC = 1.0 g/m^3 case, the ice completely accretes around the leading edge, with milky-white structures typical of rime ice. We also see the leading-edge ice thickness increase as time goes on. In Fig. 4(b), for the LWC = 3.0 g/m^3 case, the milky-white rime ice is accompanied by a thin layer of translucent mixed ice, which forms complex shapes and alters the geometry of the airfoil. We also see the leading-edge ice thickness increase as time goes on, but the total thickness is lesser, and more ice is spread out in the form of mixed ice. In Fig. 4 (c), for the LWC = 6.0 g/m^3 case, we observe much more ice accreting close to the leading edge, with more prominent translucent mixed ice formation, and a resultant decrease in the leading-edge ice thickness.

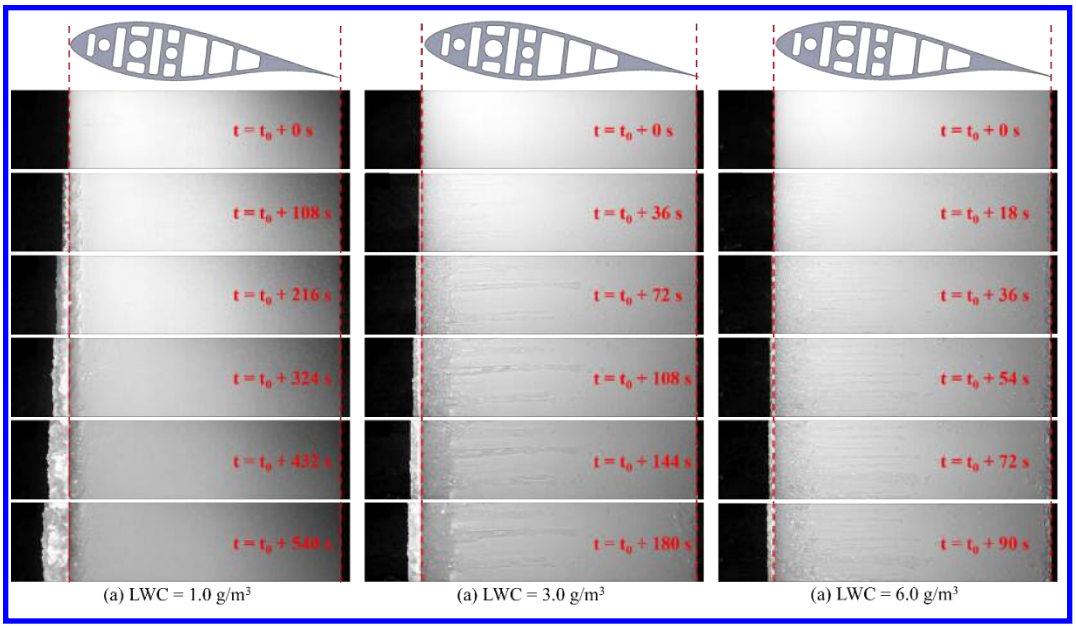

Figure 3: Dynamic ice accretion on the airfoil surface for V = 60 m/s, T = -5°C, and AoA = 8° at (a) and LWC = 1.0 g/m^3, (b) and LWC = 1.0 g/m^3, (c) and LWC = 1.0 g/m^3

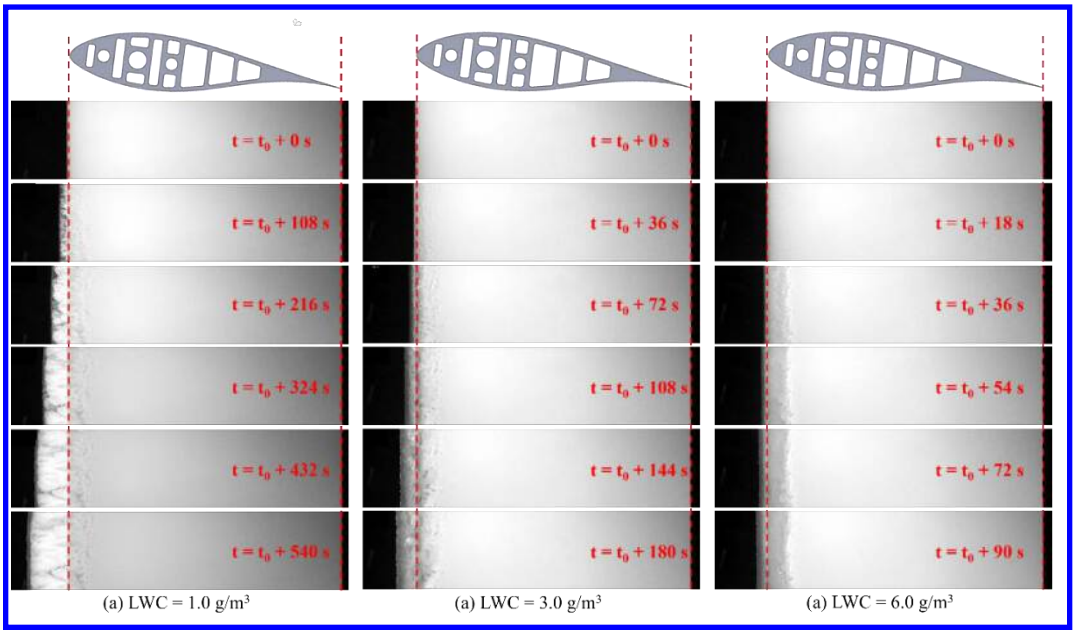

Figure 4: Dynamic ice accretion on the airfoil surface for V = 60 m/s, T = -5°C, and LWC = 3.0 g/m^3 at (a) t = 0s, (b) t = 60s, (c) t = 120s, and (d) t = 180s.

3.2 Aerodynamic Performance Degradation results

To capture the aerodynamic performance degradation due to rainfall quantitatively, two force transducers were mounted on either side of the airfoil to measure the lift and drag experienced by the airfoil. The resultant lift and drag forces were normalized using the following equation to obtain the Coefficients of Lift and Drag (C_L and C_D):

$$C_L = \frac{Lift}{\frac{1}{2}\rho V^2} \; ; \; C_D = \frac{Drag}{\frac{1}{2}\rho V^2}$$

From Fig. 5(a), we can see that the degradation of lift is the greatest for LWC = 1.0 g/m^3, followed by LWC = 3.0 g/m^3, with LWC = 6.0 g/m^3 showing the least degradation. The corresponding increase in drag follows the same trend as well, in Fig. 9(b). This can be explained by the fact that the leading-edge ice thickness decreases with an increase in the LWC value. Since the change in geometry is the most extreme when most of the ice accretes around the leading edge, the aerodynamic performance degradation also correspondingly is the worst. Fig. 6 (a) and (b) show the normalized degradation rates for the coefficients of lift and drag respectively:

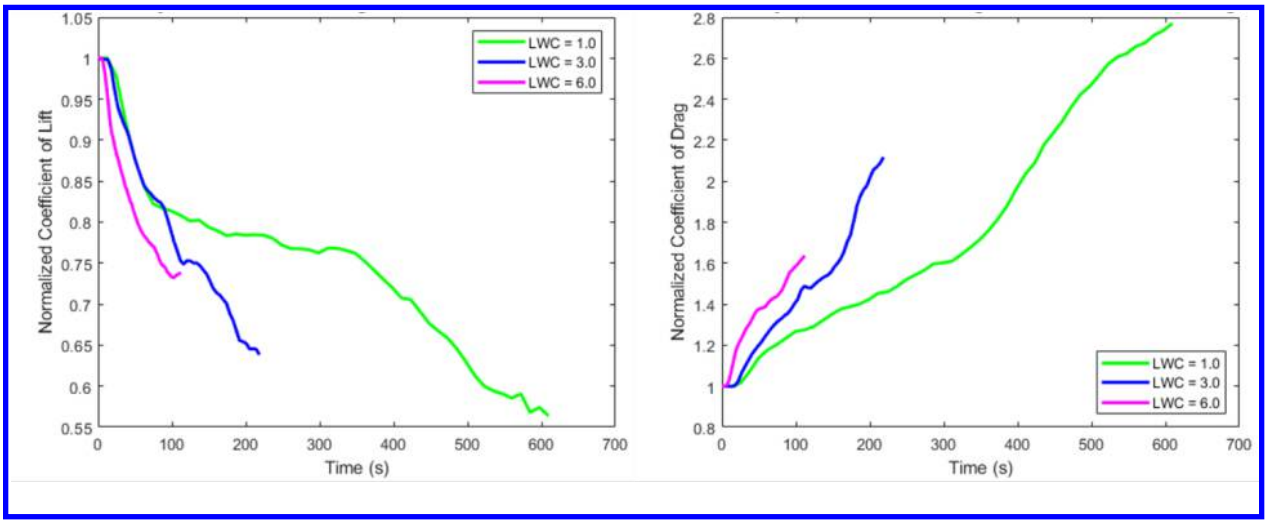

Figure 5: Aerodynamic Performance Degradation of the airfoil due to the dynamic glaze ice accretion for (a) Coefficient of Lift and (b) Coefficient of Drag

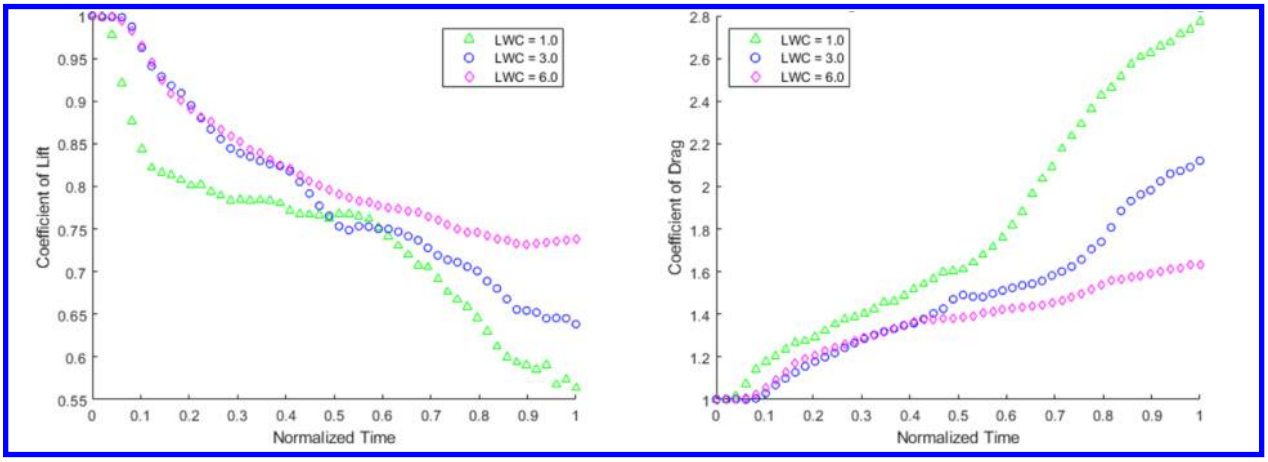

Figure 6: Normalized Aerodynamic Performance Degradation of the airfoil due to dynamic glaze ice accretion for (a) Coefficient of Lift and (b) Coefficient of Drag.

Force measurements were conducted for the rime icing cases as well. The degradation is the greatest for LWC = 3.0 g/m^3, followed by LWC = 6.0 g/m^3 and LWC = 1.0 g/m^3 as shown in Fig. 6. This deviation in the trend in terms of

the leading-edge ice thickness can be attributed to the formation of mixed ice at higher moisture levels in lower temperatures, which forms non-uniform ice structures, greatly altering the geometry of the airfoil. The normalized coefficients of lift and drag for the rime icing conditions are shown in Fig. 7:

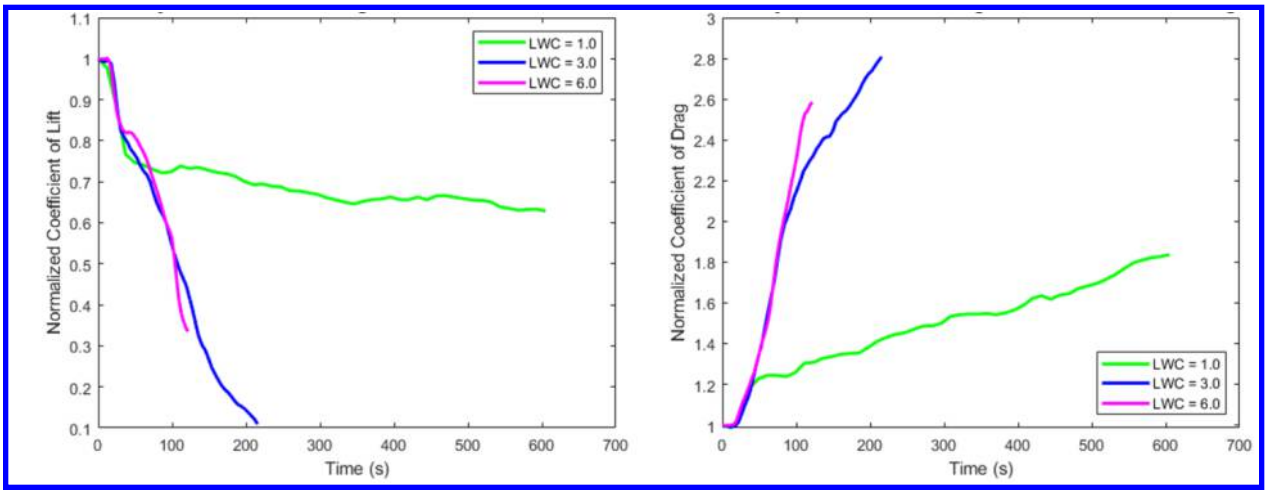

Figure 7: Aerodynamic Performance Degradation of the airfoil due to the dynamic rime ice accretion for (a) Coefficient of Lift and (b) Coefficient of Drag.

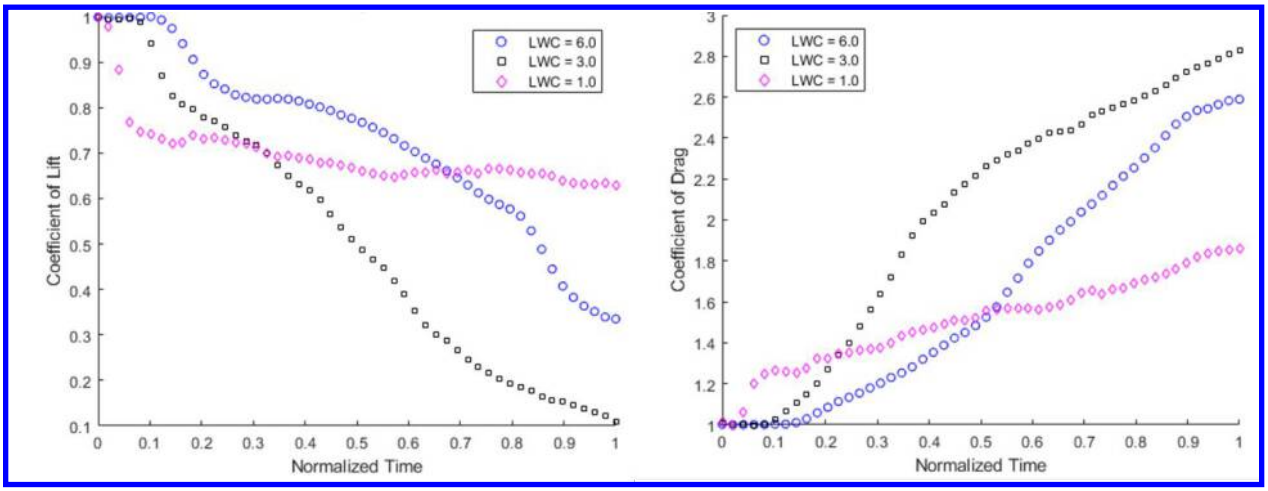

Figure 8: Normalized Aerodynamic Performance Degradation of the airfoil due to dynamic rime ice accretion for (a) Coefficient of Lift and (b) Coefficient of Drag

3.3 Particle Image Velocimetry results

The next step is to characterize the flow field around the iced airfoil using PIV. The cases with the worst degradation have been selected for PIV, i.e. LWC = 1.0 g/m^3 for glaze ice and LWC = 3.0 g/m^3 for rime ice. Since the Angle of Attack is set to 8 degrees, which is before stall for this airfoil, the baseline case should not have flow separation. However, once the ice accretion starts, flow separation occurs due to the change in the geometry and surface roughness of the airfoil. The accreted ice is shown in grey in the figures. Such premature separation is an indication of a loss in aerodynamic performance. Fig. 9 shows the dynamic PIV measurements for the glaze icing process at LWC = 1.0 g/m^3, T = -5ºC, and AoA = 8º. We see the separation layer expanding as the ice gets more severe, with significant recirculation occurring towards the end of the experiment at 432s and 540s.

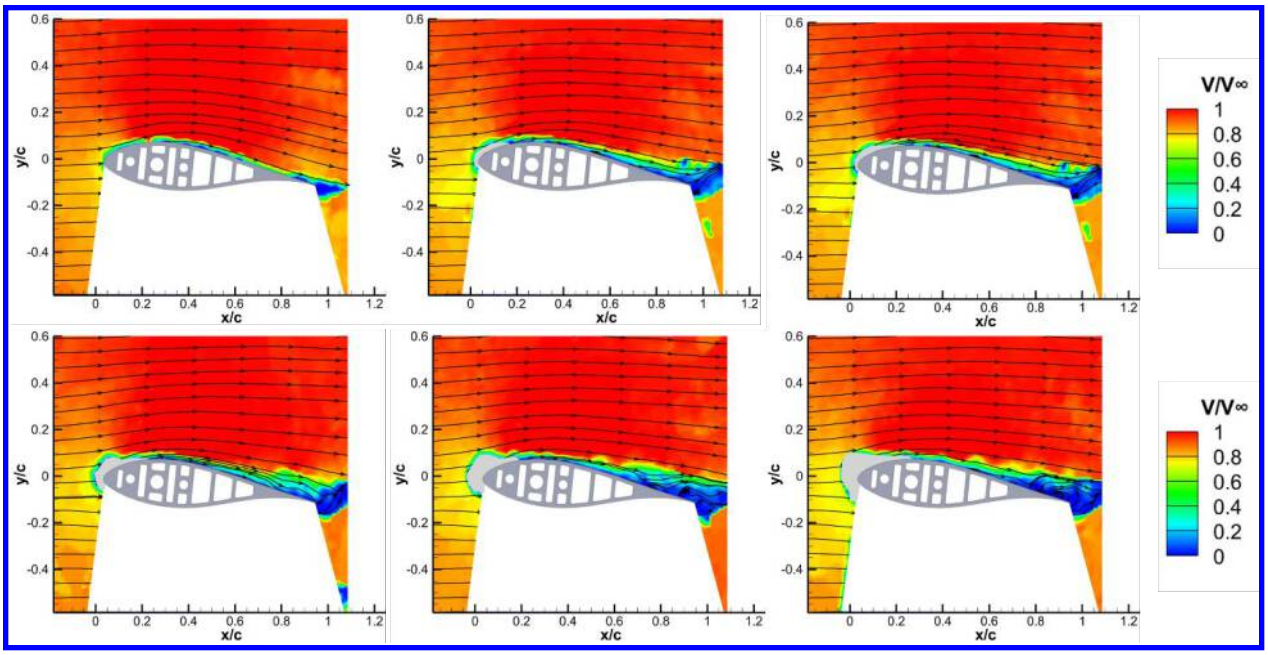

Figure 9: PIV measurements on the airfoil surface for V = 60 m/s, T = -5°C, AoA = 8°, and LWC = 1.0 g/m^3 at (a) t = 0s, (b) t = 108s, (c) t = 216s, (d) t = 324s, (e) t = 432s, and (f) t = 540s

Fig. 10 shows the dynamic PIV measurements for the rime icing process at LWC = 3.0 g/m^3, T = -15°C, and AoA = 8°. We see the separation layer expanding substantially with the mixed ice thickness, causing large recirculation regions that correspond to the force measurements discussed in Section 3.2.

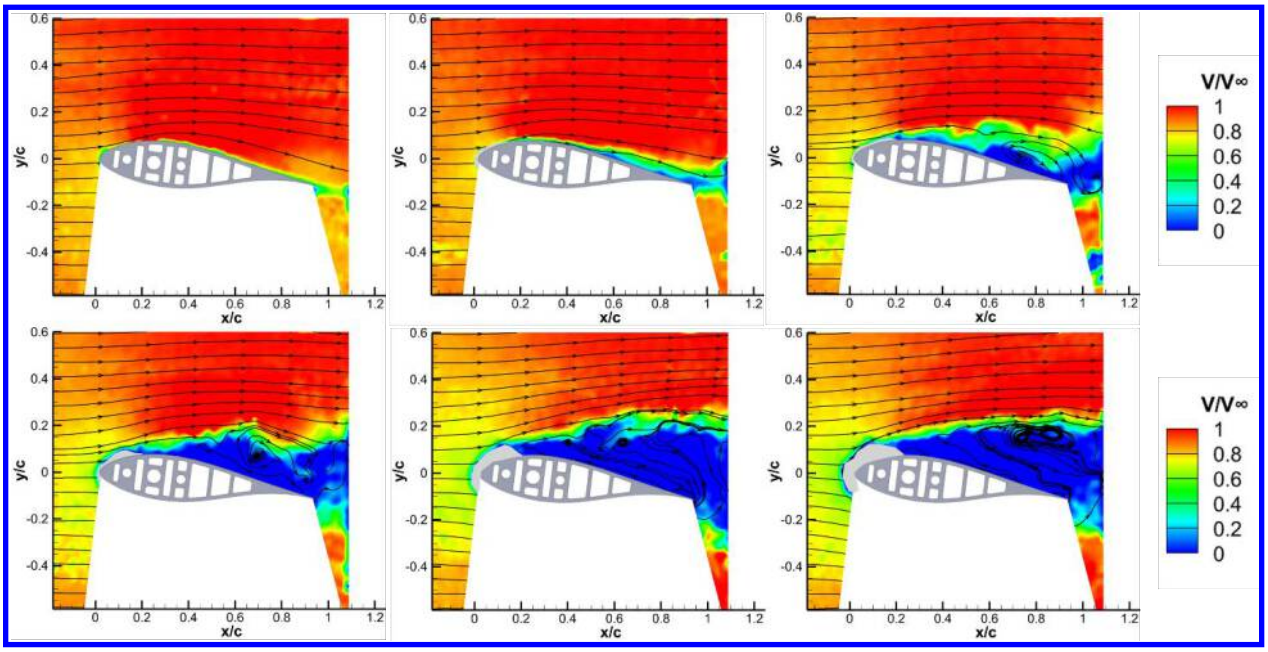

Figure 10: PIV measurements on the airfoil surface for V = 60 m/s, T = -15°C, AoA = 8°, and LWC = 3.0 g/m^3 at (a) t = 0s, (b) t = 36s, (c) t = 72s, (d) t = 108s, (e) t = 144s, and (f) t = 180s.

Overall, the separation layer is much greater for rime ice as compared to glaze ice because of the formation of mixed ice which changes the geometry of the airfoil significantly. From Section 3.2, the LWC = 1.0 g/m^3 case for glaze ice reported a 45% decrease in lift, whereas the LWC = 3.0 g/m^3 case for rime ice reported a 90% decrease in lift, which

is reflected in Fig. 9 and Fig. 10. Therefore, high LWC values at lower temperatures are the most dangerous conditions in terms of aerodynamic performance.

4. Conclusions

The present study examines the aerodynamic performance degradation due to icing on an offshore wind turbine at high Liquid Water Content (LWC) values and different ambient temperatures to cover the spectrum of glaze, mixed, and rime icing conditions. Various flow diagnostic techniques such as high-speed imaging, load cell force measurements, and Particle Image Velocimetry (PIV) have been used to experimentally characterize the flow field and quantify the performance degradation. It was found that there are different fundamental physics covering the two different regimes of icing, with the leading-edge ice thickness playing a key role for glaze icing, while mixed ice formation plays the key role for rime ice at high LWC values. The worst cases among three representative LWC values were chosen to further investigate using PIV. The lift and drag degradation measured from the load cells corresponds to the separation layer width observed in PIV. All the employed diagnostic techniques conclude that higher levels of water at low temperatures lead to the formation of dangerous mixed ice, which can decrease the aerodynamic performance of the wind turbine significantly.

Acknowledgments

The research was partially supported by the Iowa Energy Center for Wind Turbine Icing Study under the IEC Competitive Grant No. 312350 and National Science Foundation (NSF) with the Award Numbers of CBET-1935363, TIP-2140489, and CBET- 2313310.

References

[1] M. Grujicic, G. Arakere, B. Pandurangan, V. Sellappan, A. Vallejo, and M. Ozen, "Multidisciplinary design optimization for glass-fiber epoxy-matrix composite 5 MW horizontal-axis wind-turbine blades," *J Mater Eng Perform*, vol. 19, no. 8, pp. 1116–1127, Nov. 2010, doi: 10.1007/S11665-010-9596-2/FIGURES/12.

[2] "Global Offshore Wind Report 2023 - Global Wind Energy Council." Accessed: May 21, 2024. [Online]. Available: https://gwec.net/gwecs-global-offshore-wind-report-2023/

[3] "Lots of good news in offshore wind, including in the supply chain | WindEurope." Accessed: May 21, 2024. [Online]. Available: https://windeurope.org/newsroom/press-releases/lots-of-good-news-in-offshore-wind-including-in-the-supply-chain/

[4] "WINDExchange: Offshore Wind Energy." Accessed: May 21, 2024. [Online]. Available: https://windexchange.energy.gov/markets/offshore

[5] V. Lehtomäki, "Wind Energy in Cold Climates Available Technologies-report," 2016.

[6] F. Lamraoui, G. Fortin, R. Benoit, J. Perron, and C. Masson, "Atmospheric icing impact on wind turbine production," *Cold Reg Sci Technol*, vol. 100, pp. 36–49, Apr. 2014, doi: 10.1016/J.COLDREGIONS.2013.12.008.

[7] F. Feng, S. Li, Y. Li, and W. Tian, "Numerical simulation on the aerodynamic effects of blade icing on small scale Straight-bladed VAWT," *Phys Procedia*, vol. 24, pp. 774–780, Jan. 2012, doi: 10.1016/J.PHPRO.2012.02.115.

[8] L. Gao, Y. Liu, L. Ma, and H. Hu, "A hybrid strategy combining minimized leading-edge electric-heating and superhydro-/ice-phobic surface coating for wind turbine icing mitigation," *Renew Energy*, vol. 140, pp. 943–956, Sep. 2019, doi: 10.1016/J.RENENE.2019.03.112.

[9] H. Hu, L. Tian, C. Eluchie, H. Sista, and H. Hu, "Comparative Study of Using Superhydrophobic and Icephobic Surface Coatings for Aircraft Icing Mitigation," *AIAA Journal*, vol. 62, no. 4, pp. 1588–1600, Apr. 2024, doi: 10.2514/1.J063579/ASSET/IMAGES/LARGE/FIGURE8.JPEG.

[10] E. Gaertner *et al.*, "Definition of the IEA Wind 15-Megawatt Offshore Reference Wind Turbine Technical Report," 2020, Accessed: May 21, 2024. [Online]. Available: www.nrel.gov/publications.

[11] H. Sista, H. Hu, L. Tian, and H. Hu, "Qualification of Ice Accretion Characteristics on a Wind Turbine Blade Model at High Liquid Water Content Levels Pertinent to Offshore Wind Turbine Icing Phenomena," *AIAA AVIATION 2022 Forum*, 2022, doi: 10.2514/6.2022-4070.

[12] H. Sista, J. Wang, H. Hu, and H. Hu, "An Experimental Study to Characterize the Effects of Ice Accretion on the Aerodynamic Performance of an Offshore Wind Turbine Blade Model," Jun. 2023, doi: 10.2514/6.2023-3524.